J|A|C|S ARTICLES

Published on Web 05/11/2009

Molecular Recognition on a Cavitand-Functionalized Silicon Surface

Elisa Biavardi,[†] Maria Favazza,[‡] Alessandro Motta,[‡] Ignazio L. Fragalà,[‡] Chiara Massera,[§] Luca Prodi,[⊥] Marco Montalti,[⊥] Monica Melegari,[†] Guglielmo G. Condorelli,*[,‡] and Enrico Dalcanale*[,†]

Dipartimento di Chimica Organica e Industriale, University of Parma and INSTM UdR Parma, V.le G. P. Usberti 17/A, 43100 Parma, Italy, Dipartimento di Scienze Chimiche, University of Catania and INSTM UdR Catania, V.le A. Doria 6, 95100 Catania, Italy, Dipartimento di Chimica Generale ed Inorganica, Chimica Analitica, Chimica Fisica, University of Parma, V.le G. P. Usberti 17/A, 43100 Parma, Italy, and Dipartimento di Chimica "G. Ciamician", Latemar Unit University of Bologna, Via Selmi 2, 40126 Bologna, Italy

Received March 4, 2009; E-mail: enrico.dalcanale@unipr.it; guidocon@unict.it

Abstract: A Si(100) surface featuring molecular recognition properties was obtained by covalent functionalization with a tetraphosphonate cavitand (*Tiiii*), able to complex positively charged species. *Tiiii* cavitand was grafted onto the Si by photochemical hydrosilylation together with 1-octene as a spatial spectator. The recognition properties of the *Si-Tiiii* surface were demonstrated through two independent analytical techniques, namely XPS and fluorescence spectroscopy, during the course of reversible complexation−guest exchange−decomplexation cycles with specifically designed ammonium and pyridinium salts. Control experiments employing a Si(100) surface functionalized with a structurally similar, but complexation inactive, tetrathiophosphonate cavitand (*TSiiii*) demonstrated no recognition events. This provides evidence for the complexation properties of the *Si-Tiiii* surface, ruling out the possibility of nonspecific interactions between the substrate and the guests. The residual Si−O$^-$ terminations on the surface replace the guests' original counterions, thus stabilizing the complex ion pairs. These results represent a further step toward the control of self-assembly of complex supramolecular architectures on surfaces.

Introduction

The introduction of specific functions onto surfaces represents one of the major themes in contemporary chemistry. Notable examples of functional surfaces include: self-cleaning surfaces mimicking the lotus leaf,[1] gecko-foot mimetic adhesive surfaces featuring carbon nanotubes−decorated silicon wafers,[2] monolayers with control of surface wettability via electrically triggered conformational transitions,[3] high density molecular electronic memory using bistable rotaxanes as storage elements.[4] Among the several surface functions identified to be worth pursuing, molecular recognition is particularly noteworthy for its profound impact on biology and materials science. In living organisms, multiple recognition events trigger the immune system response through antibodies, and they promote the adhesion of viruses on cell surfaces.[5] In nanotechnology, the controlled positioning of molecules and assemblies on surfaces can be driven by multiple binding events.[6] Another significant field impacted by molecular recognition on surfaces is chemical sensing, in which the recognition process is translated into an analytical signal.[7]

Organic monolayers hosted on inorganic surfaces[8] represent the best approach for harnessing the full potential of molecular

[†] Dipartimento di Chimica Organica e Industriale, University of Parma and INSTM UdR Parma.

[‡] Dipartimento di Scienze Chimiche, University of Catania and INSTM UdR Catania.

[§] Dipartimento di Chimica Generale ed Inorganica, Chimica Analitica, Chimica Fisica, University of Parma.

[⊥] Dipartimento di Chimica "G. Ciamician", Latemar Unit University of Bologna.

(1) (a) Erbil, H. Y.; Demirel, A. L.; Avci, Y.; Mert, O. *Science* **2003**, *299*, 1377–1380. (b) Li, X.-M.; Reinhoudt, D. N.; Crego-Calamata, M. *Chem. Soc. Rev.* **2007**, *36*, 1350–1368.

(2) Qu, L.; Dai, L.; Stone, M.; Xia, Z.; Wang, Z. L. *Science* **2008**, *322*, 238–242.

(3) Lahann, J.; Mitragotri, S.; Tran, T.-N.; Kaido, H.; Sundaram, J.; Choi, I. S.; Hoffer, S.; Somorjai, G. A.; Langer, R. *Science* **2003**, *299*, 371–374.

(4) Green, J. E.; Choi, J. W.; Boukai, A.; Bunimovich, Y.; Johnston-Halperin, E.; DeIonno, E.; Luo, Y.; Sheriff, B. A.; Xu, K.; Shin, Y. S.; Tseng, H.-R.; Stoddart, J. F.; Heath, J. R. *Nature* **2007**, *445*, 414–417.

(5) Mammen, M.; Choi, S.-K.; Whitesides, G. M. *Angew. Chem., Int. Ed.* **1998**, *37*, 2754–2794.

(6) (a) Ludden, M. J. W.; Reinhoudt, D. N.; Huskens, J. *Chem. Soc. Rev.* **2006**, *35*, 1122–1134. (b) Ludden, M. J. W.; Mulder, A.; Tampè, R.; Reinhoudt, D. N.; Huskens, J. *Angew. Chem., Int. Ed.* **2007**, *46*, 4104–4107.

(7) (a) Lavigne, J. J.; Anslyn, E. V. *Angew. Chem., Int. Ed.* **2001**, *40*, 3118–3130. (b) Pirondini, L.; Dalcanale, E. *Chem. Soc. Rev.* **2007**, *36*, 695–706.

(8) (a) Dubey, M.; Bernasek, S. L.; Schwartz, J. *J. Am. Chem. Soc.* **2007**, *129*, 6980–6981. (b) Zhang, S.; Cardona, C. M.; Echegoyen, L. *Chem. Commun.* **2006**, 4461–4473. (c) Facchetti, A.; Annoni, E.; Beverina, L.; Morone, M.; Zhu, P.; Marks, T. J.; Pagani, G. A. *Nat. Mater.* **2004**, *3*, 910–917. (d) Liu, Z.; Yasseri, A. A.; Lindsey, J. S.; Bocian, D. F. *Science* **2003**, *302*, 1543–1545. (e) Altman, M.; Shukla, A. D.; Zubkov, T.; Evmenenko, G.; Dutta, P.; van der Boom, M. E. *J. Am. Chem. Soc.* **2006**, *128*, 7374–7382. (f) Gupta, T.; van der Boom, M. E. *J. Am. Chem. Soc.* **2006**, *128*, 8400–8401.

Chart 1. Structure of the Anchored Receptors and the Tested Guests

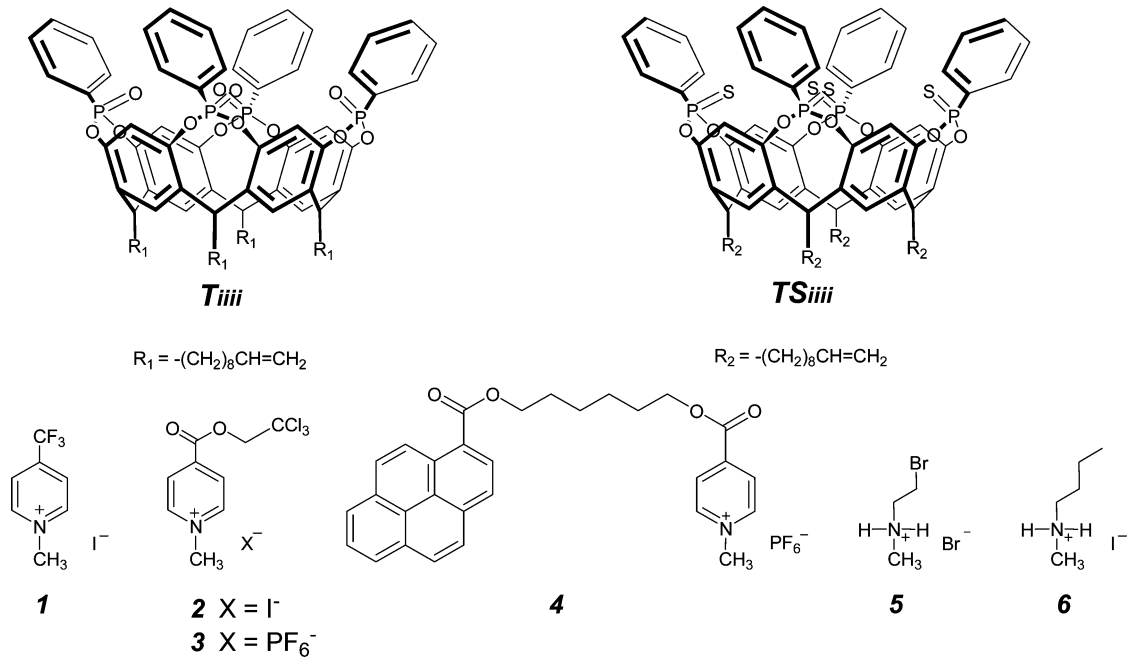

recognition on surfaces.[9] Compared to both thin films and bulk materials containing molecular receptors, such hybrid organic−inorganic materials have the advantage of reducing or even eliminating nonspecific interactions which often mask the recognition events.[10] Silicon is a particularly attractive inorganic platform, as it offers the possibility to make robust and durable devices by forming stable Si−C covalent bonds. Moreover, the grafting of molecular receptors on silicon wafers represents an important step toward the generation of silicon-integrated devices.

Phosphorus-bridged cavitands[11] are a promising class of synthetic molecular receptors. The introduction of four P(V) stereogenic centers as bridging units creates a family of six diastereomeric cavitands, each with a different orientation of the P=O groups, i.e. inward (i) or outward (o) with respect to the cavity.[12] Among these molecules, tetraphosphonate cavitands with an all-inward configuration[13] (Chart 1) are particularly versatile in their ability to complex positively charged species, such as inorganic cations,[14]ammonium and pyridinium salts,[15] as well as neutral molecules such as alcohols.[16] This diverse complexation ability is the result of three interaction modes, which can be activated either individually or in combination by the host according to the guest requirements. These include (i) multiple ion−dipole interactions between the inward facing P=O groups and the positively charged guests,[14] (ii) single or multiple H-bonding involving the P=O groups,[14,17] and (iii) $CH_3-\pi$ interactions between an acidic methyl group present on the guest and the π-basic cavity of the host.[16] Depending on the type and number of interactions activated, the measured K_{ass} in nonpolar solvents can vary between 10^2 M^{-1} for short-chain alcohols to 10^9-10^{10} M^{-1} for *N*,*N*-methylalkylammonium salts.[15b,18]

We recently published a protocol for the covalently assembly of cavitands on silicon surface,[19] along with various aspects of the coordination chemistry of the resulting cavitand-decorated assemblies.[20] In the current study we report a comprehensive investigation of the molecular recognition properties of a silicon surface decorated with phosphonate cavitands toward methylpyridinium and methylammonium guests. The entire process, consisting of methylpyridinium complexation, guest exchange with methylammonium salts, base-driven decomplexation of the latter accompanied by restoration of the initial complex, is fully reversible. Each step of the process was monitored using two independent techniques, namely X-ray photoelectron spectroscopy (XPS) and fluorescence spectroscopy. Control experiments with a silicon surface covered with a structurally similar, yet

(9) (a) Descalzo, A. B.; Martìnez-Màòez, R.; Sancenòn, F.; Hoffmann, K.; Rurack, K. *Angew. Chem., Int. Ed.* **2006**, *45*, 5924–5948. (b) Lagrost, C.; Alcaraz, G.; Bergamini, J.-F.; Fabre, B.; Serbanescu, I. *Chem. Commun.* **2007**, 1050–1052.
(10) For a clearly defined example of the influence of non specific interactions on the sensing performances of cavitand layers see: Tonezzer, M.; Melegari, M.; Maggioni, G.; Milan, R.; DellaMea, G.; Dalcanale, E. *Chem. Mater.* **2008**, *20*, 6535–6542.
(11) (a) Dutasta, J.-P. *Top. Curr. Chem.* **2004**, *232*, 55–91. (b) Pinalli, R.; Suman, M.; Dalcanale, E. *Eur. J. Org. Chem.* **2004**, 451–462. (c) Nifantyev, E. E.; Maslennikova, V. I.; Merkulov, R. V. *Acc. Chem. Res.* **2005**, *38*, 108–116. (d) Puddephatt, R. J. *Can. J. Chem.* **2006**, *84*, 1505–1514.
(12) (a) Lippmann, T.; Mann, G.; Dalcanale, E. *Tetrahedron Lett.* **1994**, *35*, 1685–1688. (b) Lippmann, T.; Wilde, H; Dalcanale, E.; Mavilla, L.; Mann, G.; Heyer, U.; Spera, S. *J. Org. Chem.* **1995**, *60*, 235–242.
(13) Delangle, P.; Dutasta, J.-P. *Tetrahedron Lett.* **1995**, *36*, 9325–9328.
(14) Delangle, P.; Mulatier, J.-C.; Tinant, B.; Declercq, J.-P.; Dutasta, J.-P. *Eur. J. Org. Chem.* **2001**, 3695–3704.
(15) (a) De Zorzi, R.; Dubessy, B.; Mulatier, J.-C.; Geremia, S.; Randaccio, L.; Dutasta, J.-P. *J. Org. Chem.* **2007**, *72*, 4528–4531. (b) Biavardi, E.; Battistini, G.; Montalti, M.; Yebeutchou, R. M.; Prodi, L.; Dalcanale, E. *Chem. Commun.* **2008**, 1638–1640.
(16) Melegari, M.; Suman, M.; Pirondini, L.; Moiani, D.; Massera, C.; Ugozzoli, F.; Kalenius, E.; Vainiotalo, P.; Mulatier, J.-C.; Dutasta, J.-P.; Dalcanale, E. *Chem.−Eur. J.* **2008**, *14*, 5772–5779.
(17) Kalenius, E.; Moiani, D.; Dalcanale, E.; Vainiotalo, P. *Chem. Commun.* **2007**, 3865–3867.
(18) Yebeutchou, R. M.; Tancini, F.; Demitri, N.; Geremia, S.; Mendichi, R.; Dalcanale, E. *Angew. Chem., Int. Ed.* **2008**, *47*, 4504–4508.
(19) Condorelli, G. G.; Motta, A.; Favazza, M.; Fragalà, I. L.; Busi, M.; Menozzi, E.; Dalcanale, E. *Langmuir* **2006**, *22*, 11126–11133.
(20) Busi, M.; Laurenti, M.; Condorelli, G. G.; Motta, A.; Favazza, M.; Fragalà, I. L.; Montalti, M.; Prodi, L.; Dalcanale, E. *Chem.−Eur. J.* **2007**, *13*, 6891–6898.

Table 1. XPS Atomic Composition Analysis of (a) HF Freshly Etched Surface, (b) Pure **Si-Tiiii** Monolayers, (c) Mixed ($\chi = 0.2$) **Si-Tiiii/Oct** Monolayers (d) Pure **Si-TSiiii** Monolayers, (e) Mixed ($\chi = 0.2$) **Si-TSiiii/Oct** Monolayers. Data Are Obtained at a 10° Electron Takeoff Angle with Respect to the Sample Surface

	Si 2p	O 1s	C 1s	P 2p	**S 2s**
HF etched	77.0	7.8	15.2	–	
pure **Si-Tiiii**	15.0	17.3	65.0	2.7	
Si-Tiiii/Oct $\chi = 0.2$	15.9	16.0	61.2	2.0	
pure **Si-TSiiii**	15.0	14.2	66.0	2.7	2.1
Si-TSiiii/Oct $\chi = 0.2$	12.5	9.4	74.3	2.1	**1.6**

complexation inactive, thiophosphonate cavitand[18] further validated the entire complexation cycle.

The active monolayer is constituted by a tetraphosphonate cavitand *Tiiii*[$C_{10}H_{19}$, *H, Ph*][21] with decyl feet (thereafter *Tiiii*, Chart 1) anchored on H-terminated Si(100) surfaces via photochemical hydrosilylation of the double bonds.[22] This same procedure was likewise used to graft the control monolayer containing tetrathiophosphonate cavitand *TSiiii*[$C_{10}H_{19}$, *H, Ph*] (thereafter *TSiiii* Chart 1). Trifluoro-, trichloro-, and bromo-marked guests **1**, **2**, **3**, **5** were specifically designed and prepared for XPS detection, while the methylpyridinium guest **4** contains pyrene as fluorescent probe.

Results and Discussion

Cavitand-Functionalized Si Surface. Cavitand grafting through photochemical hydrosilylation was optimized according to a previous study.[19] Pure and mixed monolayers of cavitands with 1-octene (*Oct*) as spectator spacer were prepared. The use of the *Oct* spectator spacer in the mixed monolayers improves the passivation of the Si surface, thus minimizing substrate oxidation due to aging.[19] Mixed *Si-Tiiii/Oct* and *Si-TSiiii/Oct* surfaces were prepared by Si grafting of 1:4 cavitand/Oct mixtures (cavitand mole fraction $\chi = 0.2$).

The elemental depth distribution and the bonding states of the *Si-Tiiii/Oct* and *Si-TSiiii/Oct* monolayers were characterized by XPS analyses. Table 1 compares the elemental compositions obtained at 10° takeoff angle of (a) a HF etched surface, (b) pure *Si-Tiiii* monolayers, (c) mixed ($\chi = 0.2$) *Si-Tiiii/Oct* monolayers (d) pure *Si-TSiiii* monolayers, and (e) mixed ($\chi = 0.2$) *Si-TSiiii/Oct* monolayers.

These data reveal an enhancement of the C 1s and O 1s signals as compared to the freshly etched silicon surface. This enhancement, together with the observation of P 2p signal, and, for the *Si-TSiiii/Oct* monolayers, an S 2s signal, indicates the presence of cavitand molecules on the silicon surface.

The high resolution C 1s region (Supporting Information Figure S1) of *Si-Tiiii* and *Si-TSiiii* grafted monolayers (pure and mixed) always included two main components: (i) a C^0 component at 285.0 eV, due to the aliphatic and aromatic hydrocarbon backbone;[23,25] and (ii) a C^{1+} component at 286.4 eV, due to the aromatic carbons bearing the bridging oxygens of the resorcinarene skeleton. No significant dependence of the

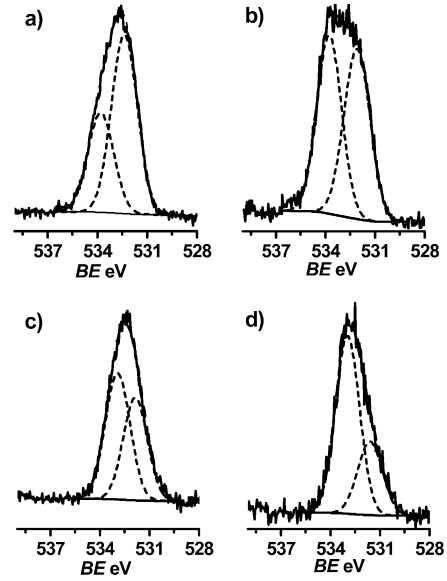

Figure 1. High-resolution O 1s spectra from pure *Si-Tiiii*. a) 45° electron takeoff angle b) 10° electron takeoff angle and from pure *Si-TSiiii*. c) 45° electron takeoff angle d) 10° electron takeoff angle.

intensity ratio of these components ($I_{C^{+1}}/I_{C^0}$) upon the electron takeoff angle has been observed in angular resolved XPS experiments. This is compatible with the position of the oxidized carbons between the aryl and alkyl moieties (both responsible of the C^0 signals) on the upper rim and the bottom feet of the cavitands, respectively (Chart 1). Moreover, one should note that additional contributions to these two components are always present due to adventitious hydrocarbons and the Si−O−C framework.[19]

The O1s band (Figure 1) of a pure silicon surface with covalently assembled *Si-Tiiii* monolayer consists of two main components centered at 533.5 eV (O_{cav}) and at 532.5 eV (O_{SiOx}). They are due to, respectively, phosphorus-bonded oxygen atoms of the cavitand and the SiOx formed from partial oxidation of the substrate. As expected for a carbonaceous overlayer on the silicon substrate, the O_{SiOx} component decreases at low takeoff angles, while the O_{cav} component increases at low takeoff angles. This behavior is consistent with the expected grafting of the cavitand feet on the silicon surface, leaving the P=O bridges at the upper rim significantly distant from the surface oxide. Similar trends are observed for the mixed *Si-Tiiii /Oct* monolayers and for the *Si-TSiiii* analogues (Figure 1).

The presence of the P 2p band is indicative of the presence of *Tiiii* and *TSiiii* cavitands on the surface. In this context, a clear distinction of phosphorus on silicon signals is not trivial, as the 2p and 2s bands of the phosphorus nearly overlap with plasmon loss bands of the silicon. To obtain a clear spectrum and a rigorous quantification of the P concentration, it is necessary to acquire XPS measurements at low takeoff angles.

(21) For the nomenclature adopted for phosphonate cavitands see reference 11b.

(22) (a) Terry, J.; Linford, M. R.; Wigren, C.; Cao, R.; Pianetta, P.; Chidsey, C. E. D. *Appl. Phys. Lett.* **1997**, *71*, 1056–1058. (b) Sung, M. M.; Kluth, G. J.; Yauw, O. K.; Maboudian, R. *Langmuir* **1997**, *13*, 6164–6168. (c) Sun, Q.-Y.; de Smet, L. C. P. M.; van Lagen, B.; Giesbers, M.; Thüne, P. C.; van Engelenburg, J.; de Wolf, F. A.; Zuilhof, H.; Sudhölter, E. J. R. *J. Am. Chem. Soc.* **2005**, *127*, 2514–2523. (d) Cerofolini, G. F.; Galati, C.; Reina, S.; Renna, L.; Condorelli, G. G.; Fragalà, I. L.; Giorgi, G.; Sgamellotti, A.; Re, N. *Appl. Surf. Sci.* **2005**, *246*, 52–67.

(23) (a) Cerofolini, G. F.; Galati, C.; Reina, S.; Renna, L.; Viscuso, O.; Condorelli, G. G.; Fragalà, I. L. *Mater. Sci. Eng., C* **2003**, *23*, 989–994. (b) Cerofolini, G. F.; Galati, C.; Reina, S.; Renna, L. *Mater. Sci. Eng., C* **2003**, *23*, 253–257. (c) Condorelli, G. G.; Motta, A.; Fragalà, I. L.; Giannazzo, F.; Raineri, V.; Caneschi, A.; Gatteschi, D. *Angew. Chem., Int. Ed.* **2004**, *43*, 4081–4084.

(24) Briggs, D. In *Practical Surfaces Analysis*, 2nd ed.; Briggs, D., Seah, M. P., Eds.; WILEY-VCH: Weinheim, Germany, 1995; Vol. 1, p 444.

(25) Beamson, G.; Briggs, D. In *High Resolution XPS of Organic Polymers*; The Scienta ESCA300 Database; Wiley & Sons: New York, 1992.

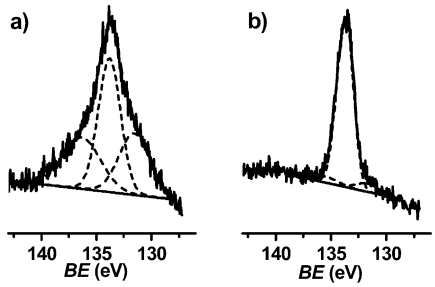

Figure 2. Typical angular dependence of high-resolution P 2p spectra from *Si-Tiiii* monolayer. a) 45° electron takeoff angle b) 10° electron takeoff angle. The tentative deconvolution reported in a) shows band overlapping.

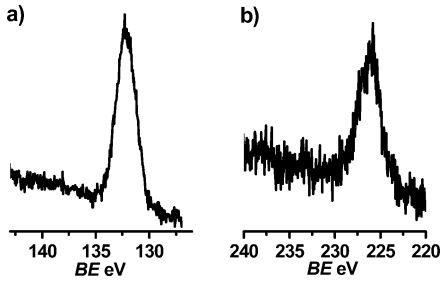

Figure 3. a) P 2p region and b) S 2s region from *Si-TSiiii* monolayer at 10° electron takeoff angle.

In fact, the substrate plasmon loss contribution decreases at low takeoff electron angles and becomes negligible at 10° (Figure 2b).

In the XPS spectrum of *Si-TSiiii*, along with the presence of the P 2p band (Figure 3a), the presence of S 2p and S 2s signals clearly demonstrate the grafting of *TSiiii*. Overall, the S 2s XPS region (Figure 3b) provides clearer information compared to the S 2p band, which partially overlaps with a plasmon loss band of the Si substrate.

The atomic ratio (P/O/C) of pure *Si-Tiiii* was inferred from the intensity of the P 2p signal obtained at a 10° takeoff angles, along with the O_{cav} component of the O 1s band and the C 1s signal (Table 1). The measured 1 /3.1/24.1 ratio is very close to the theoretical value of 1/3/23 expected from the molecular structure. The analogous P/O/C ratio observed for mixed *Si-Tiiii* is more carbon-rich (1/3.2/30.7), as expected when grafting from a mixed *Tiiii /Oct* ($\chi = 0.2$) solution (solution atomic ratio: 1/3/31).

Similarly, the P/S/O/C ratios estimated by XPS for pure and mixed *Si-TSiiii* (1/0.8/2.4/24.3 and 1/0.8/2.5/35.5, respectively) are consistent with the expected values calculated from pure *TSiiii* (1/1/2/23) and from the mixed *Tiiii/Oct* ($\chi = 0.2$) grafting solution (1/1/2/31).

Crystal Structure of the Tiiii[C_2H_5, H, Ph]•1 Complex. The reported crystal structure reveals in the solid state the interaction modes between guest **1** and *Tiiii[C_2H_5, H, Ph]* (the short feet version of the grafted cavitand, Figure 4a). The inclusion of **1** into the cavity is driven by strong dipolar interactions between the positively charged nitrogen atom and the P=O groups of *Tiiii* (the shortest distance for P=O···N^+ is 2.845(5) Å). Further stabilization is provided by a C−H···π interaction between a methyl hydrogen of the cation and an aromatic ring of the cavity (the C−H···centroid distance is of 3.575(2) Å, with an angle of 158.46(1)°). The iodide counterion is located below the cavity at 1.904(1) Å from the least-squares plane defined by the four CH_2 carbons, roughly in the middle of the four alkyl chains at the lower rim. This position is stabilized by C−H···I^- interactions with the CH_2 groups of the chains, which range in length from 3.077(1) to 3.246(1) Å. The distance between I^- and the positive nitrogen of the guest is of 8.743(6) Å. All the above values are in good agreement with previously reported findings in the literature.[15a,26] This represents the optimal arrangement for the counterion in order both to stabilize the ion-pair and to experience aliphatic CH-anion interactions. The localization of the iodide counterion is important not only for the stabilization of the complex in solution, but also for the surface complexation mode (as it will be discussed later).

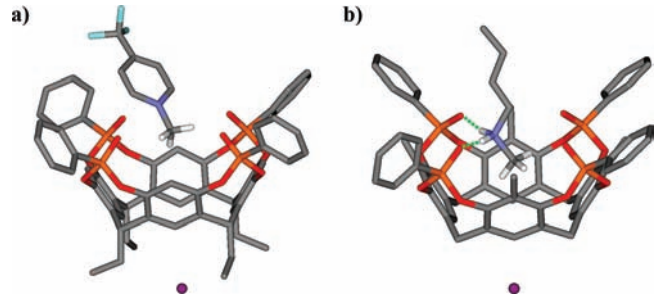

Figure 4. Molecular structures of a) *Tiiii[C_2H_5, H, Ph]•1* and b) *Tiiii[H, CH_3, Ph]•6*. H-bonding in structure b is represented by green dots. Only the H atoms involved in interactions are shown. In the case of complex b the solvent molecules and the second orientation of guest **6** are not shown.

Crystal Structure of the Tiiii[H, CH_3, Ph]•6 Complex. A second crystal structure was pursued to demonstrate the presence of H-bonding interactions between the tetraphosphonate cavitands and the secondary ammonium ions in the solid state. Solution[15b] and gas phase[17] data already indicate that H-bonding interactions strongly enhance complexation in the case of protonated ammonium salts. However, structural evidence of the number and geometry of these H-bonding interactions is currently lacking. The crystal structure of *Tiiii[H, CH_3, Ph]•6* complex reported here fills this gap (Figure 4b). The cavitand receptor employed here does not bear alkyl chains at the lower rim. In the complex, two hydrogen bonds are present between adjacent P=O and the NH_2 protons (dotted green lines in Figure 4b). The NH_2 moiety of the guest is disordered over two positions, each showing an occupancy factor of 0.5. This allows the formation of two sets of energetically and geometrically equivalent hydrogen bonds, which increase the entropic stabilization of the complex (see SI for details). Further stabilization is provided by several C−H···π interactions among the N-CH_3 hydrogens and the aromatic rings of the cavity (the C−H···centroids distances span from 2.923(9) to 2.992(9) Å and the angles span from 136.6(3) to 147.4(4)°). Due to the disorder of the nitrogen, also the methyl hydrogens adopt two different orientations. The iodide counterion is located below the cavity at 3.188(3) Å from the least-squares plane defined by the four CH_2 carbon atoms of the lower rim, roughly aligned with the cation in the cavity (in the *Tiiii[C_2H_5, H, Ph]•1* complex this value is 3.449(2) Å). This is the optimal position of the iodide counterion in the solid state, independent from the presence of alkyl chains at the lower rim. The distance between I^- and the disordered nitrogen atom of the guest is of 7.199(6) Å (N1) and of 7.269(9) Å (N1′). These values indicate that the guest in the *Tiiii[H, CH_3, Ph]•6* complex is located deeper within the cavity, with respect to the

(26) Mansikkamäki, H.; Nissinen, M.; Rissanen, K. *Chem Commun.* **2002**, 1902–1903.

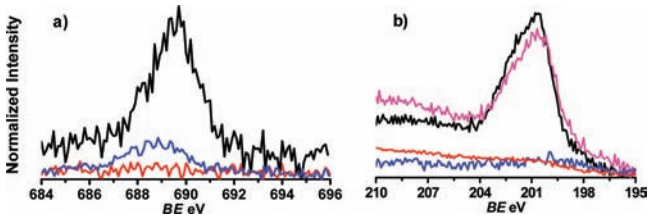

Figure 5. a) F 1s XPS region of *Si-TSiiii/Oct* after complexation with guests **1** (red curve), *Si-Tiiii/Oct* before complexation (blue curve) and *Si-Tiiii/Oct* complexed with guest **1** (black curve); b) Cl 2p XPS regions of *Si-TSiiii/Oct* after complexation with guests **2** and **3** (red curve), *Si-Tiiii/Oct* before complexation tests (blue curve); *Si-Tiiii/Oct* complexed with guest **2** (pink curve) and *Si-Tiiii/Oct* complexed with guest **3** (black curve).

Tiiii[C_2H_5, *H, Ph*]•*1* case, drawn in by the formation of the two H-bonds. Therefore, the reported crystal structures validate the higher affinity of *Tiiii* cavitands for N,N-methylalkyl ammonium salts over methylpyridinium salts.

Complexation on Si-surface: XPS Detection. The affinity of the *Si-Tiiii* toward guests **1**−**3** was evaluated by XPS. The guests were specifically functionalized with three halogen atoms to allow for XPS quantification. The Cl 2p and F 1s peaks were monitored as the main indicators of guest complexation; they have a significant advantage with respect to the other pyridinium bands (namely N 1s at 402 eV, and C 1s component at 289.6 eV) in that they are located in a less crowded spectral region and possess a higher intensity. Complexation was performed by treating both mixed ($\chi = 0.2$) *Si-Tiiii/Oct* (active sensing) and mixed ($\chi = 0.2$) *Si-TSiiii/Oct* (control experiment) substrates with guests **1**−**3** (10^{-3} M solution in CH_2Cl_2 for **1** and in CH_3CN for **2** and **3**).

Figure 5 compares the F 1s and the Cl 2p regions of mixed ($\chi = 0.2$) *Si-Tiiii/Oct* and *Si-TSiiii/Oct* after the complexation reaction with either (a) guest **1** or (b) guests **2** and **3**. Precomplexation spectra are also reported for reference. The presence of halogen bands in the *Si-Tiiii/Oct* grafted samples follwing exposure to the guests demonstrates surface complexation. At the same time, the absence of halogen signals for inert *Si-TSiiii/Oct* precludes the possibility of physisorption, due to nonspecific interactions between the charged guest and the surface.

An interesting observation regards the role played by the counterions: in all cases, no significant signals were observed for the I^- and PF_6^- counterions. The kinetics of iodide disappearance on the surface was monitored via XPS for guest **2**. Immediately following exposure of the surface to the guest, the I $3d_{5/2}$ signal was observed. After several minutes, however, the intensity of the signal began to decrease, disappearing entirely in about one hour (see Figures S2 and S3, SI).

The counterions, positioned between the alkyl chains as indicated by the crystal structures, are sufficiently close to the surface to react with the residual Si-OH surface terminations. The reaction leads to the formation of HF plus PF_5 in the case of guest **3**, and HI in the case of guests **1** and **2**. These molecules are sufficiently volatile to escape from the surface. The $Si-O^-$ terminations on the surface become the new counterions of the *Si-Tiiii* complexes, sufficiently close to the guest to stabilize the ion-pair (Figure 6). This anion replacement by a charged surface is unexpected and unprecedented.

XPS analyses allowed to estimate the efficiency of host−guest complexation. In this context, the chlorine-marked guests **2** and **3** are better probes than guest **1**, both to monitor the success of the complexation and to evaluate quantitatively its

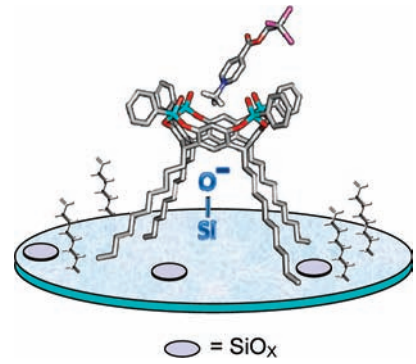

Figure 6. Proposed ion-pair formation for *Si-Tiiii* complexes on the silicon surface.

efficiency. This is due to the fact that the presence of chlorine, unlike fluorine, cannot be confused with contaminants resulting from the HF etching process.

Given the 1:1 stoichiometry of all the complexes reported, the theoretical atomic ratio between P and Cl for the complexed species is 3/4. Hence, the efficiency of complexation (i.e., yield of the complex formed) on the surface can be calculated as follows:

$$\text{Yield of complexation } \% = \frac{\% \text{ Cl}}{\% \text{ P}} / \frac{3}{4} \times 100$$

The complexation yield was estimated in the range 60− 70% for both guests **2** and **3**. Similar results were obtained for guest **5** (see next paragraph). No remarkable differences were observed by changing the solvent. The independence of surface complexation from both the guest and solvent nature, together the lower efficiency compared to solution data, suggests that the binding is related to the percentage of surface bonded cavitands whose cavity is available for complexation.

Complexation on Si-surface: Fluorescence Detection. To confirm the complexation properties of *Si-Tiiii/Oct* silicon surface, we synthesized a pyridinium salt connected to a pyrene probe via a diester tether.[15b] Guest **4** has the peculiar property of activating the fluorescence emission of this pyrene probe upon complexation. The inclusion of the electron-poor methylpyridinium moiety within the electron-rich cavity of *Tiiii* decreases the exoergonicity of the electron-transfer process from pyrene to the methylpyridinium unit, leading to a thirty-fold increase in fluorescence emission.[15b] Figure 7 (curve a) shows the typical structure of the fluorescence band of the pyrene moiety with $\lambda_{max} = 384$ nm for the *Si-Tiiii/Oct* complexed with guest **4**. No signal is evident for *Si-TSiiii/Oct* under the same conditions. These data validate the XPS results, i.e. pyridinium salts are captured on the surface only in the presence of the *Tiiii* cavities. Moreover, the absence of the excimeric band in spectra (a) and (c) indicates that the complexes on the surface are isolated and not clustered.

Molecular Recognition on Si-surface: Reversible Guest Exchange. Considering the potential application of tetraphosphonate cavitand-decorated silicon surfaces as sensor elements in integrated devices, a fundamental issue to be addressed regards the capability of these systems to perform reversible guest exchange processes. The reversibility of the association process was tested by performing cyclic guest exchange between methylpyridinium and *N,N*-methylalkyl ammonium salts. The proposed complexation cycle replicates the one previously studied by us in solution, monitored via fluorescence spectroscopy.[15b] XPS measurements were used

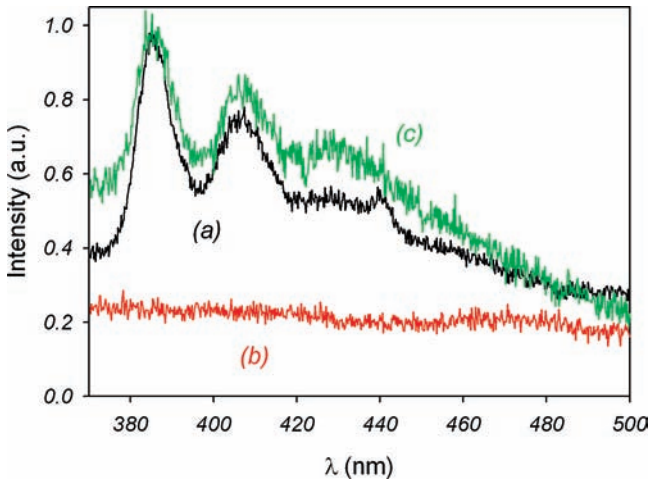

Figure 7. Fluorescence spectra of: (a) *Si-Tiiii/Oct* surface after complexation test with guest **4**, (b) after addition of the ammonium ion **6**, and (c) after treatment with DBU and subsequent treatment with a solution of **4**. The spectrum resulting from a pristine *Si-Tiiii/Oct* surface is superimposable to curve (b).

to monitor the steps of this cycle, specifically by tracking the presence of the chlorine-marked guest **2** and the bromine-marked guest **5**.

The *Si-Tiiii/Oct•2* surface (henceforth referred to as *Si-Tiiii•2*), was taken as the starting point of the cycle; it shows a prominent signal in the Cl 2p region (as described above) and, obviously, no signal in the Br 3d region (Figure 8a). After treatment of *Si-Tiiii•2* with a solution of guest **5** (10^{-3} M in CH_3CN), a negligible signal is present in the Cl 2p region, while the Br 3d region presents an evident Br 3d signal (Figure 8b). These results are diagnostic of the exchange of the guest **2** with the guest **5** in the cavity of the tetraphosphonate cavitand, forming the *Si-Tiiii•5* system. On silicon, as in solution, the higher affinity of the guest **5** for tetraphosphonate cavitands[15b,18] drives the exchange process. The obtained complexation yield expressed as $Yield = (\%Br)/(\%P)/(1)/(4) \times 100$ was similar (70%) to that calculated for guests **2** and **3**.

Treatment of the *Si-Tiiii•5* surface with a hindered Brønsted base (such as 1,8-diazabicyclo[5.4.0]undec-7-ene, DBU; 10^{-3} M in CH_3CN), led to complete removal of guest **5** from the surface, as demonstrated by the absence of both halogen signatures in Cl 2p and Br 3d regions (Figure 8c).

DBU, by extracting a proton from guest **5**, induces the dissociation of the *Si-Tiiii•5* complex, restoring the pristine *Si-Tiiii* surface. Exposure of the resulting *Si-Tiiii* surface to a solution of guest **2** led to the original *Si-Tiiii•2* complex (Figure 8d). Figure 9 illustrates the fully reversible cycle consisting of (i) the complexation of the guest **2**, (ii) the exchange of **2** with the protonated guest **5**, and (iii) the regeneration of the original surface by removal of guest **5** with DBU.

The same complexation cycle was monitored by fluorescence spectroscopy using guests **4** and **6**, respectively (Figure 10). In this case, the addition of the guest **6** to the *Si-Tiiii•4* system (Figure 7, trace a) led to the complete disappearance of the fluorescence signal on the surface, due to the formation of fluorescence silent complex *Si-Tiiii•6* (Figure 7, trace b). Addition of DBU, followed by the treatment of the silicon surface with a solution of **4**, restored the initial fluorescent *Si-Tiiii•4* complex (Figure 7, trace c).

The combination of XPS and fluorescence spectroscopy provides a consistent and reliable picture of the three consecutive recognition steps (complexation, guest exchange, and decomplexation) occurring on the surface of a *Si-Tiiii* wafer.

Conclusion

In this paper, we have described the preparation, characterization, and molecular recognition properties of a functional surface featuring phosphonate cavitands as receptors. The relevant findings can be summarized as follows: (i) The photochemical hydrosilylation protocol is compatible with the presence of P=O/P=S bridging units on the cavitands, allowing the formation of both pure and mixed monolayers on the silicon surface. The mixed monolayers improve the coverage of the surface, minimizing substrate oxidation. (ii) The noteworthy molecular recognition properties of this class of synthetic receptors were successfully transferred to a technologically relevant silicon platform. (iii) The preferential positioning of the counterions between the alkyl chains at the lower rim allows for their replacement by the $Si-O^-$ groups generated on the surface.

A unique feature of this study has been the possibility to record independent sets of measurements by monitoring the surface complexation experiments with two different techniques, namely XPS and fluorescence spectroscopy. The resulting cross validation provides a highly reliable, comprehensive picture of the complexation cycle on the *Si-Tiiii* surface. Moreover, control experiments with the structurally similar, but complexation inactive, *Si-TSiiii* surface excluded the possibility of nonspecific interactions between the substrate and the guests. The sequence complexation−guest exchange−decomplexation demonstrated that all three interaction modes of the host available for complexation are operative on the silicon surface without interference. In particular, the two additional H-bonds experienced by guests **5** and **6** upon complexation, inferred from the crystal structure, are sufficient to induce the complete guest exchange on the *Si-Tiiii* surface. Removal of these guests by deprotonation resets the original surface cleanly and efficiently.

Besides sensing[16] and synthetic applications,[27] the functional surface described in this work represents a useful addition to the available pool of molecular printboards for the self-assembly of complex supramolecular architectures on surfaces.[6] Orthogonality of the *Si-Tiiii* interaction mode with the H-bonding motifs for the layer-by-layer assembly on silicon has likewise been demonstrated in our lab, and it will be reported in due course.

Experimental Section

Materials. Cavitands *Tiiii*[$C_{10}H_{19}$, *H, Ph*],[28] *Tiiii*[C_2H_5, *H, Ph*][29] and *Tiiii*[*H,* CH_3, *Ph*][10] and guests **1**[30] and **4**[15b] were prepared following published procedures. The syntheses of the phosphonate cavitand *Tiiii*[C_2H_5, *H, Ph*], thiophosphonate cavitand *TSiiii*[$C_{10}H_{19}$, *H, Ph*], and guests **2**, **3**, **5**, **6** are described in detail in the Supporting Information.

Crystal Structures. The crystal structure of the complexes *Tiiii*[C_2H_5, *H, Ph*]·$CF_3C_5H_4NCH_3^+I^-$ and *Tiiii*[*H,* CH_3, *Ph*]·

(27) Yebeutchou, R. M.; Dalcanale, E. *J. Am. Chem. Soc.* **2009**, *131*, 2452–2453.
(28) Bibal, B.; Tinant, B.; Declercq, J.-P.; Dutasta, J.-P. *Supramol. Chem.* **2003**, *15*, 25–32.
(29) Cantadori, B.; Betti, P.; Boccini, F.; Massera, C.; Dalcanale, E. *Supramol. Chem.* **2008**, *20*, 29–34.
(30) Timperley, C. M.; Bird, M.; Heard, S. C.; Notman, S.; Read, R. W.; Tattersall, J. E. H.; Turner, S. R. *J. Fluorine Chem.* **2005**, *126*, 1160–1165.

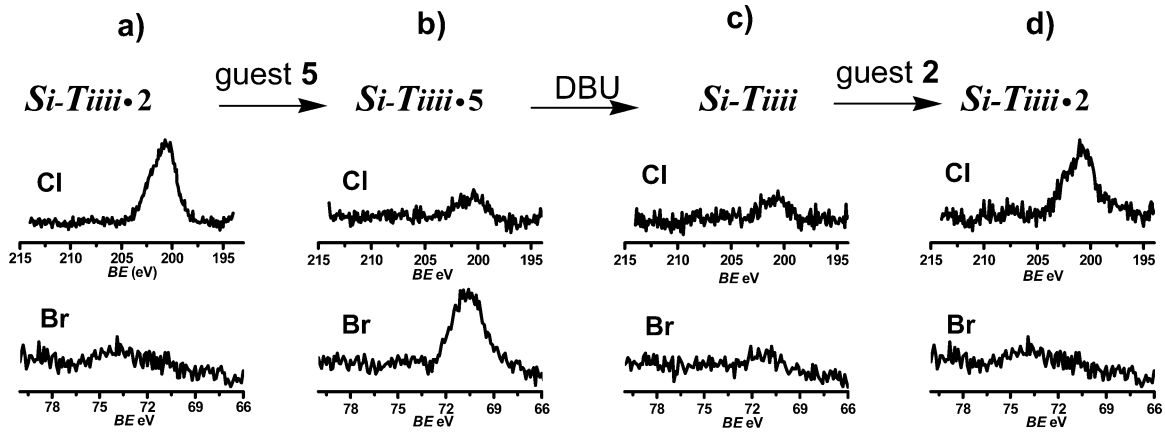

Figure 8. Cl 2p and Br 3d XPS region after treatment of the *Tiiii*-grafted silicon surface with a) a solution of guest **2**, b) a solution of guest **5**, c) a solution of DBU, and d) a solution of guest **2**, again.

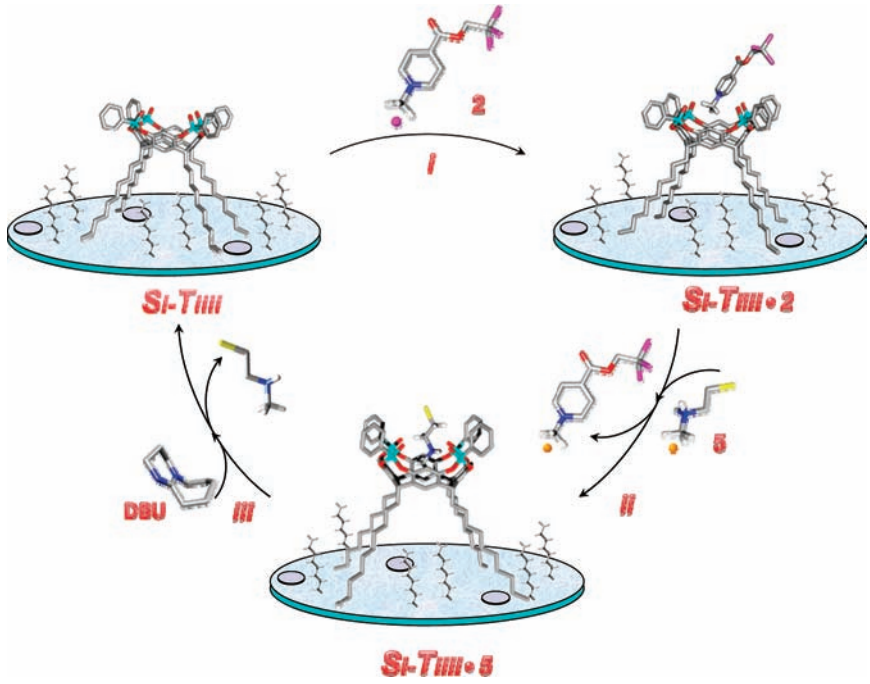

Figure 9. Complexation cycle of *Si-Tiiii*, as monitored by XPS. The Si−O$^-$ counterions are omitted for clarity.

$C_4H_9NH_2CH_3^+I^-$ were determined by single crystal X-ray diffraction methods. Crystallographic and experimental details for the structures are summarized in Table S1 in the Supporting Information. Intensity data and cell parameters were recorded at room temperature for *Tiiii*$[C_2H_5$, *H, Ph*$]\cdot CF_3C_5H_4NCH_3^+I^-$ and at 173 K for *Tiiii*$[H, CH_3$, *Ph*$]\cdot C_4H_9NH_2CH_3^+I^-$ on a Bruker AXS Smart 1000 single-crystal diffractometer, equipped with a CCD area detector using graphite monochromated Mo Kα radiation. The structures were solved by direct methods using the SIR97 program[31] and refined on F_o^2 by full-matrix least-squares procedures, using the SHELXL-97 program.[32] Both programs were used in the WinGX suite.[33] The data reduction was performed using the SAINT[34] and SADABS[35] programs. The PLATON SQUEEZE procedure[36] was used to treat regions of diffuse solvent which could not be sensibly modeled in terms of atomic sites. Their contribution to the diffraction pattern was removed and modified F_o^2 written to a new HKL file. The number of electrons thus located, 191 per unit cell, are included in the formula, formula weight, calculated density, μ and $F(000)$. This residual electron density was assigned to six molecules of acetone solvent per unit cell (six molecules of acetone would give 192 e).

All the non-hydrogen atoms were refined with anisotropic atomic displacements, with the exclusion of one of the fluorine atoms of the guest **1**, of two carbon atoms of the guest **6** and of one carbon atom of the phenyl group in the *Tiiii*$[H, CH_3$, *Ph*$]$ host. The hydrogen atoms were included in the refinement at

(31) Altomare, A.; Burla, M. C.; Camalli, M.; Cascarano, G. L.; Giacovazzo, C.; Guagliardi, A.; Moliterni, A. G. G.; Polidori, G.; Spagna, R. *J. Appl. Crystallogr.* **1999**, *32*, 115–119.
(32) Sheldrick, G. M. *SHELXL97, Program for Crystal Structure Refinement*; University of Göttingen: Göttingen, Germany, 1997.
(33) WinGX: Farrugia, L. J. *J. Appl. Crystallogr.* **1999**, *32*, 837–838.
(34) *SAINT, Software Users Guide, 6.0*; Bruker Analytical X-ray Systems: Madison, WI, 1999.
(35) Sheldrick, G. M. *SADABS Area-Detector Absorption Correction, 2.03*; University of Göttingen: Göttingen, Germany, 1999.
(36) SQUEEZE: Sluis, P. V. D.; Spek, A. L. *Acta Crystallogr., Sect. A* **1990**, *46*, 194–201.

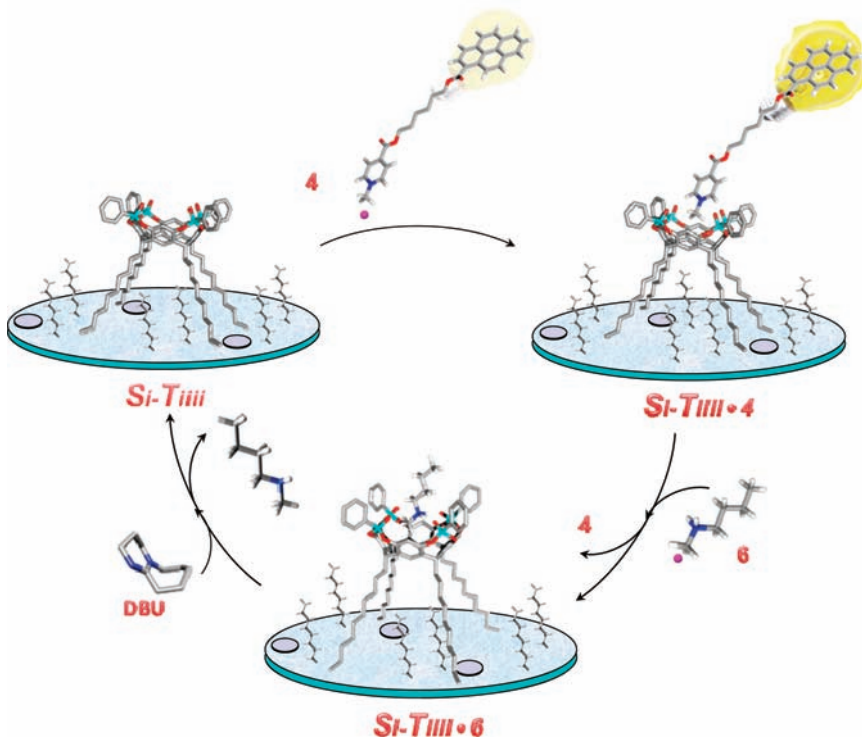

Figure 10. Complexation cycle of *Si-Tiiii,* as monitored by fluorescence. The Si−O$^-$ counterions are omitted for clarity.

idealized geometries (C−H 0.95 Å) and refined "riding" on the corresponding parent atoms. In the guest **6**, the nitrogen atom was found disordered over two positions, each showing an occupancy factor of 0.5. The weighting scheme used in the last cycle of refinement was $w = 1/[\sigma^2F_o^2 + (0.0865P)^2 + 0.7176P]$ and $w = 1/[\sigma^2F_o^2 + (0.0927P)^2]$ where $P = (F_o^2 + 2F_c^2)/3$, for *Tiiii*[C_2H_5, *H, Ph*]·$CF_3C_5H_4NCH_3^+I^-$ and *Tiiii*[*H*, CH_3, *Ph*]·$C_4H_9NH_2CH_3^+I^-$, respectively. CCDC-731069 and -731070 contain the supplementary crystallographic data. These data can be obtained free of charge at www.ccdc.cam.ac.uk/conts/retrieving.html [or from the Cambridge Crystallographic Data Centre, 12 Union Road, Cambridge CB2 1EZ, UK; Fax: +44-1223/336-033]. Geometric calculations were performed with the PARST97 program.[37]

Cavitand Grafting on Si. For grafting monolayers, pure cavitand ($\chi_{cav} = 1.0$) and cavitand/1-octene mixtures ($\chi_{cav} = 0.2$) were dissolved in mesitylene (solution concentration = 0.05 M). Cavitand solutions (2.0 mL) were placed in a quartz cell and deoxygenated by stirring in a drybox for at least 1 h. A Si(100) substrate was dipped in H_2SO_4/H_2O_2 (3:1) solution for 12 min to remove organic contaminants, then it was etched in a hydrofluoric acid solution (1% v/v) for 90 s and quickly rinsed with water. The resulting hydrogenated silicon substrate was immediately placed in the mesitylene solution. The cell remained under UV irradiation (254 nm) for two hours. The sample was then removed from the solution and sonicated in dichloromethane for 10 min to remove residual physisorbed material.

Cavitand Complexation Tests. To test the complexation properties of *Si-Tiiii* and *Si-TSiiii*, samples were dipped in a solution 10^{-3} M of guests **1**−**6** in CH_3CN for 30 min and then sonicated in CH_3CN for 10 min. The same treatment was followed for the DBU decomplexation.

XPS Characterizations. The XPS spectra were run with a PHI ESCA/SAM 5600 Multy technique spectrometer equipped with a monochromated Al Kα X-ray source, a standard dual-anode Mg/Al source and a spherical capacitor analyzer (SCA) with a mean diameter of 279.4 mm. The analyses were carried out at various photoelectron angles (relative to the sample surface) in the 10°−80° range with an acceptance angle of ±7° (the acceptance angle was fixed high to avoid photoelectron diffraction effects).

Atomic concentrations have been evaluated from the intensity of both standard Mg and monochromatic Al spectra after removing of a Shirley background and correction for the Wagner sensitivity factors.[38] All high-resolution XPS spectra were recorded adopting only monochromatic Al radiation. Experimental uncertainties in binding energies lie within ±0.28 eV.[39] Some spectra were deconvoluted by fitting the spectral profiles with a series of symmetrical Gaussian envelopes after subtraction of the background. The agreement factor, $R = [\Sigma(F_o - F_c)^2/\Sigma-(F_o)^2]^{1/2}$, after minimization of the function $\Sigma(F_o - F_c)^2$ converged to R values ≤0.04. XPS B.E. scale was calibrated by centering the C 1s peak of the adventitious carbon at 285.0 eV.[40,41]

Fluorescence Measurements. Fluorescence spectra on *Si-Tiiii* and *Si-TSiiii* surfaces were obtained using a spectrofluorimeter ISA FLUOROLOG 3 in a front-face geometry, with a He−Cd continuum laser at 325 nm, 50 mW power, as excitation source.

Acknowledgment. This paper is dedicated to Prof. J. Rebek, Jr. on the occasion of his 65th birthday. This work has been supported by the EU through NoE MAGMANet (3-NMP 515767-2), MIUR through FIRB 2003-2004 LATEMAR (http://www.latemar.polito.it) (B.O.), INSTM through PRISMA "Mo-

(37) Nardelli, M. *J. Appl. Crystallogr.* **1996**, *29*, 296–300.
(38) Wagner, C. D.; Davis, L. E.; Zeller, M. V.; Taylor, J. A.; Raymond, R. H.; Gale, L. H. *Surf. Interface Anal.* **1981**, *4*, 211–225.
(39) (a) Cerofolini, G. F.; Galati, C.; Renna, L.; Viscuso, O.; Camalleri, M.; Lorenti, S.; Condorelli, G. G.; Fragalà, I. L. *J. Phys. D.: Appl. Phys.* **2002**, *35*, 1032–1038. (b) Cerofolini, G. F.; Galati, C.; Renna, L. *Surf. Interface Anal.* **2002**, *34*, 583–589.
(40) Swift, I. L. *Surf. Interface Anal.* **1982**, *4*, 47–51.
(41) Cerofolini, G. F.; Galati, C.; Lorenti, S.; Renna, L.; Viscuso, O.; Bongiorno, C.; Raineri, V.; Spinella, C.; Condorelli, G. G.; Fragalà, I. L.; Terrasi, A. *Appl. Phys. A: Mater. Sci. Process.* **2003**, *77*, 403–409.

lecular systems grafted on silicon for integrated sensing devices". The instrumental facilities at the Centro Interfacoltà di Misure G. Casnati of the University of Parma were utilized. We thank Dr. M. Busi for growing X-ray quality crystals of one phosphonate complex.

Supporting Information Available: Preparation and characterization of host *TSiiii* and guests **2**, **3**, **5**, **6**; high-resolution XPS measurements and kinetics; X-ray crystallographic data and CIF files; ORTEP drawing of the two crystal structures. This material is available free of charge via the Internet at http://pubs.acs.org.

JA901678B